

# PromptReverb: Multimodal Room Impulse Response Generation Through Latent Rectified Flow Matching

Ali Vosoughi<sup>3†‡</sup>, Yongyi Zang<sup>1†</sup>, Qihui Yang<sup>2†</sup>, Nathan Peak<sup>4†</sup>, Randal Leistikow<sup>1</sup>, Chenliang Xu<sup>3</sup>

<sup>1</sup>Smule Labs <sup>2</sup>University of California, San Diego <sup>3</sup>University of Rochester <sup>4</sup>Stanford University

<sup>†</sup>Work done during internship at Smule, <sup>‡</sup>These authors contributed equally.

Room impulse response (RIR) generation remains a critical challenge for creating immersive virtual acoustic environments. Current methods suffer from two fundamental limitations: the scarcity of full-band RIR datasets and the inability of existing models to generate acoustically accurate responses from diverse input modalities. We present *PromptReverb*, a two-stage generative framework that addresses these challenges. Our approach combines a variational autoencoder that upsamples band-limited RIRs to full-band quality (48 kHz), and a conditional diffusion transformer model based on rectified flow matching that generates RIRs from descriptions in natural language. Empirical evaluation demonstrates that *PromptReverb* produces RIRs with superior perceptual quality and acoustic accuracy compared to existing methods, achieving 8.8% mean RT60 error compared to –37% for widely used baselines and yielding more realistic room-acoustic parameters. Our method enables practical applications in virtual reality, architectural acoustics, and audio production where flexible, high-quality RIR synthesis is essential.



## 1 Introduction

The pursuit of seamless virtual experiences across VR, gaming, and remote collaboration increasingly demands perceptually convincing environments that extend beyond visual fidelity to encompass spatial audio, which establishes presence through room impulse responses (RIRs) that encode sound propagation from source to listener (Liang et al., 2024). Despite RIRs’ crucial role in enabling realistic audio synthesis through convolution with dry signals, their generation remains fundamentally constrained by the trade-off between computational tractability and perceptual quality.

Traditional physics-based approaches, including ray tracing and image-source models (Allen and Berkley, 1979; Krokstad et al., 1968; Zhao et al., 2025; Liu et al., 2025; Lyu et al., 2025), provide physically accurate simulation but require detailed geometric and material specifications while remaining computationally intractable at high frequencies necessary for real-time applications. This computational burden has motivated a shift toward learning-based methods that bypass explicit physics simulation. Image2Reverb (Singh et al., 2021) pioneered single-image RIR synthesis but remains critically dependent on depth estimation accuracy, while recent multi-modal approaches such as AV-RIR (Ratnarajah et al., 2024) and MEAN-RIR (Zhang et al., 2025) achieve superior accuracy through panoramic imagery fusion, yet require specialized 360° capture equipment impractical for consumer deployment. Parametric alternatives like FAST-RIR (Ratnarajah et al., 2022b) and geometry-dependent MESH2IR (Ratnarajah et al., 2022a) offer computational efficiency but demand either precise acoustic parameter specification or detailed 3D meshes, respectively, creating significant barriers to accessibility.

Beyond computational and input constraints, existing approaches face two critical limitations preventing practical deployment. First, the scarcity of high-quality, full-band RIR datasets severely constrains model training; most datasets contain either band-limited recordings (often below 24 kHz) with paired multimodal descriptions, or synthetic RIRs from physics simulation that fail to capture real acoustic complexity. This directly impacts perceptual quality, particularly in high-frequency content crucial for spatial localization and timbral accuracy. Second, despite recent

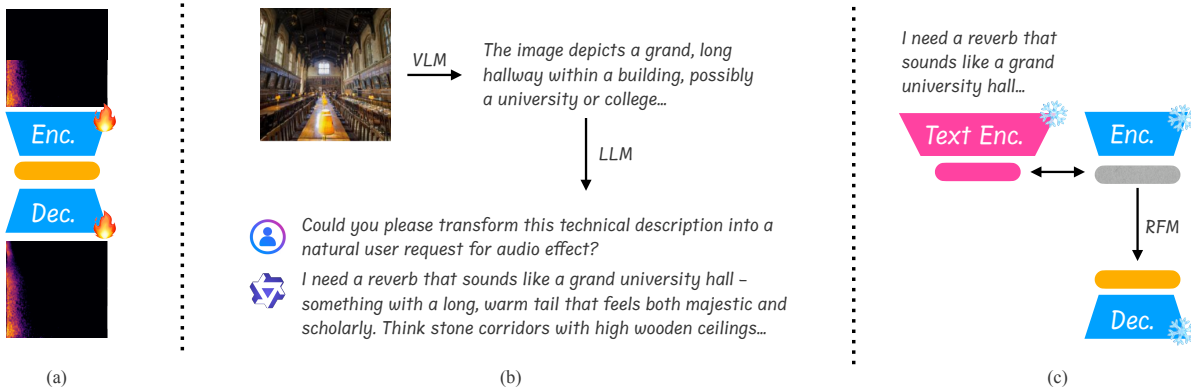


**Figure 1** **PromptReverb** system. **(a)** A VAE pretraining stage that learns an encoder (Enc.) to produce compact latent representations and a decoder (Dec.) to upsample all impulse responses to 48 kHz; **(b)** A caption-then-rewrite pipeline that employs vision-language models (VLM) to generate descriptions of visual scenes, followed by large language models (LLM) that transform these descriptions into diverse textual prompts; **(c)** A latent rectified flow matching (RFM) model that generates reverb characteristics in the latent space, conditioned on the text descriptions produced in stage (b).

diffusion-based methods for RIR completion or interpolation (de la Torre et al., 2024; Lin et al., 2024), no existing approach supports natural language conditioning for complete RIR generation, which is crucial for creative use. Current text-based systems either require technical parameter specification (Arellano et al., 2025) or operate as modification tools within manually selected parametric constraints (Richter-Powell et al., 2025), rather than enabling intuitive, free-form textual control over acoustic properties.

In this work, we present *PromptReverb*, a two-stage generative framework that addresses these fundamental limitations through architectural decoupling: (1) a variational autoencoder (VAE) that performs neural upsampling from band-limited to full-band RIRs (48 kHz), enabling us to leverage existing band-limited datasets while producing perceptually complete outputs, and (2) a conditional diffusion transformer based on rectified flow matching (Liu et al., 2022a) with transformer architectures (Peebles and Xie, 2023) that generates band-limited RIRs from natural language descriptions. To create diverse textual training data without manual annotation, we developed a caption-then-rewrite pipeline leveraging vision language models for initial scene description followed by LLM-based creative rewriting.

Through empirical evaluation, we demonstrate that our system achieves 8.8% mean RT60 error compared to 37% for existing baselines when conditioned on natural language descriptions, representing the first method to synthesize complete RIRs from free-form textual input while eliminating requirements for panoramic captures, depth estimation, 3D geometry, or acoustic parameter specification.<sup>1</sup>

## 2 Method

We decompose PromptReverb into three components, demonstrated in Fig. 1: a VAE that learns and decodes a compact full-band RIR latent (Sec. 2.1), a caption-then-rewrite pipeline that yields natural-language conditioning from images (Sec. 2.2); and a conditional rectified-flow Diffusion Transformer (DiT) that generates RIR latents from multimodal inputs using the frozen VAE decoder (Sec. 2.3).

### 2.1 Variational Autoencoder

We train a reverb variational autoencoder (VAE) that operates on mono impulse responses to learn compact latent representations. Our architecture employs ResBlocks (He et al., 2016) as the encoder, processing complex-valued spectrograms projected onto 128 mel-scaled bands of the input impulse responses. For the decoder, we adopt a hybrid architecture combining 1D ConvNeXt blocks (Liu et al., 2022b) with a preprocessing stage of Transformer (Peebles and Xie, 2023; Vaswani et al., 2017), following the WavTokenizer (Ji et al., 2024). The encoder employs a downsampling

<sup>1</sup> Audio examples are available at <https://ali-vosoughi.github.io/PromptReverb/>.

stride factor of  $[1, 2, 3]$  on temporal axis, yielding a compact latent representation with dimensionality 16 and temporal resolution of 23.6 Hz. For a standard five-second impulse response, this configuration produces 118 latent frames.

We train VAE following the  $\beta$ -VAE framework (Higgins et al., 2017) with  $\beta = 10^{-4}$ , incorporating adversarial training using HiFi-GAN discriminators (Kong et al., 2020). Our total loss function comprises three components: a reconstruction loss computed on the Mel-spectrogram domain combined with the mean absolute error of RT60 values (Singh et al., 2021), a Hinge GAN adversarial loss for improved perceptual quality, and a feature matching loss computed on intermediate discriminator feature maps. During training, we randomly reduce the sample rate for input audio, yet ask the decoder to still output full-band impulse response, thereby training it to be able to perform upsampling natively. This allows us to train the latent DiT model using only 22 kHz impulse response, yet still get full-band generation quality.

## 2.2 Caption-Then-Rewrite Pipeline

We begin by captioning images from (Singh et al., 2021) using two vision-language models (VLM): Moondream2 2B (Voleti et al., 2024) and Qwen2-VL 72B Instruct (Wang et al., 2024). For Moondream2, we utilized its native captioning API directly. For Qwen2-VL, we designed a structured prompt requesting five acoustic-relevant fields: *SPACE TYPE*, *SIZE CLASS*, *MAIN MATERIALS*, *SOFT COVERAGE*, and *RT60 BUCKET*, taking advantage of a large language backbone’s extended reasoning ability and world knowledge.

To determine which description style better supports creative rewriting, we employed an LLM-as-a-judge evaluation with a 5-model panel: Gemini 2.5 Pro (Comanici et al., 2025), GPT-4o (OpenAI, 2024a), GPT-5 (OpenAI, 2024b), Claude Opus 4.1 (Anthropic, 2024), and Mistral Medium 3.1 (Mistral AI, 2024). Each judge performed pairwise comparisons between Qwen2.5-VL-72B (Wang et al., 2024) and Moondream2 (Voleti et al., 2023) descriptions using the prompt: “*Which image description is better for creative rewriting?*” Judges provided structured responses in `\boxed{A}` or `\boxed{B}` format, which we extracted via regular expressions. We evaluated 100 randomly sampled description pairs with randomized A/B positioning to prevent order bias. The panel reached near-unanimous consensus through majority voting, and to our surprise, the much smaller Moondream2 descriptions are preferred in 99.8% of cases with exceptional inter-judge agreement. Despite this finding, we still opt to include Qwen2-VL’s captioning results in, as we believe they provide key acoustic details for the space to guide generation.

Following VLM captioning, we employ Microsoft Phi-4 14B (Research, 2024) to transform factual descriptions into diverse natural user requests through multi-dimensional randomization. Our rewriting framework operates across several axes of variation to ensure comprehensive diversity in the generated prompts.

We incorporate 50+ distinct writing styles, spanning from “*casual and conversational*” through “*poetic and atmospheric*” to “*technical and precise*”, ensuring broad linguistic coverage. We implement 40+ user personas representing diverse use cases, including “*musician recording their first album*”, “*experienced podcaster with millions of listeners*”, and “*voice actor preparing for an animated film*”, capturing the heterogeneous nature of real-world RIR applications. Each generation follows structured templates that guide naturalistic transformation, such as “*Transform this technical description into a natural user request for audio effects*” and “*Convert this factual room description into how someone would ask for that acoustic sound*”. The system randomly selects conversational starters (“*Hey*,” “*I’d love*,” “*Could you*,” “*I’m hoping*,” “*Please*,” “*Can you help me*”) and appends emotional contexts (“*– it’s really important to me*,” “*because it brings back memories*,” “*to capture that perfect mood*”) to enhance authenticity.

For each image, we generate 55 creative prompts, including long and short prompt versions. We randomize temperature  $\in [0.6, 1.2]$  and top-p  $\in [0.8, 0.98]$  to balance creativity with coherence, ensuring linguistic diversity across generated prompts. The methodology successfully transforms technical specifications like “*large concert hall; large; plaster, wood, upholstered-seats; 20; long (1.8 s)*” into authentic user requests such as “*Hey, I need my audio to sound like it was recorded in a grand concert hall with that beautiful long reverb tail - it’s really important to me*,” bridging the gap between acoustic parameters and natural language expression.

## 2.3 Rectified Flow Matching

We train a DiT with conditional rectified flow matching (Liu et al., 2022a) to learn the transformation from noise to RIR latents. The model learns a velocity field  $v_\theta(\mathbf{x}_t, t, c)$  that transports Gaussian noise samples  $\mathbf{x}_0 \sim \mathcal{N}(0, I)$  to RIR latent representations  $\mathbf{x}_1$  along optimal straight-line trajectories defined by  $\mathbf{x}_t = (1 - t)\mathbf{x}_0 + t\mathbf{x}_1$  for  $t \in [0, 1]$ . This

transport follows the ordinary differential equation:

$$\frac{d\mathbf{x}}{dt} = v_\theta(\mathbf{x}_t, t, c), \quad (1)$$

where  $c$  represents multimodal conditioning including text embeddings, audio features, and constant parameters.

The training objective employs a flow-matching loss with pseudo-Huber penalty for improved gradient stability:

$$\begin{aligned} \mathcal{L}_{\text{FM}} &= \mathbb{E}_{t, \mathbf{x}_0, \mathbf{x}_1, c} [L_\delta(v_\theta(\mathbf{x}_t, t, c) - (\mathbf{x}_1 - \mathbf{x}_0))] , \\ L_\delta(\mathbf{z}) &= \delta^2 \left( \sqrt{1 + \|\mathbf{z}/\delta\|_2^2} - 1 \right) , \end{aligned} \quad (2)$$

where we set  $\delta = 1.0$  per coordinate, matching the typical velocity scale in  $\mathbf{x}_1 - \mathbf{x}_0$ . This parameterization remains invariant to data-parallel training strategies and GPU configurations.

To enable classifier-free guidance (CFG) during inference, we implement dropout-based conditioning augmentation during training, replacing  $c$  with learned unconditional embeddings  $c_{\text{uncond}}$  with probability 0.2. At inference, we apply CFG with scale 6.0 to enhance conditioning adherence:

$$\begin{aligned} v_{\text{guided}} &= v_\theta(\mathbf{x}_t, t, c_{\text{uncond}}) \\ &+ 6.0 (v_\theta(\mathbf{x}_t, t, c) - v_\theta(\mathbf{x}_t, t, c_{\text{uncond}})) . \end{aligned} \quad (3)$$

For generation, we integrate the learned ODE using an adaptive midpoint solver (RK2) with maximum 50 function evaluations and tolerance  $\text{rtol} = \text{atol} = 10^{-5}$ . We apply cosine time reparameterization  $t \mapsto \tau(t) = \frac{1-\cos(\pi t)}{2}$  during both training and sampling phases to improve convergence dynamics.

## 3 Experiments

### 3.1 Dataset

We assembled a large RIR dataset comprising 145,976 training, 7,964 validation, and 1,957 test samples, each standardized to 5-second duration. Our corpus integrates diverse acoustic environments from multiple established sources: C4DM (Stewart and Sandler, 2010), RIRS NOISES (Ko et al., 2017), Image2Reverb (Singh et al., 2021), synthetic RIRs generated via PyRoomAcoustics (Scheibler et al., 2018), SoundSpaces 2.0 RIRs (Chen et al., 2022), and OpenAIR (Murphy, 2010). To enhance acoustic diversity beyond conventional spaces, we augmented the dataset with manually collected free-license RIRs from online forums, including unconventional environments such as “RIR of inside a large glass fishbowl helmet<sup>2</sup>”.

The complete training set of 145,976 samples was utilized to maximize acoustic diversity during model training. For multi-channel RIRs, we randomly select one channel at each training iteration.

### 3.2 Objective Experiments

**Text Encoder for Conditioning.** To identify optimal text encoding strategies for capturing acoustic semantics, we evaluated 15+ text encoders with varying pooling strategies. We investigated multiple pooling approaches: mean pooling (averaging across sequence dimension), maximum pooling (element-wise maximum across sequences), first-token extraction (utilizing the initial token representation), last-token pooling, and hybrid combinations. Our evaluation tested each configuration on 15 prompts spanning small intimate spaces to large concert halls. We assess encoder quality through three complementary metrics: (1) *Batch Diversity*, measuring mean per-dimension standard deviation across the batch using raw embeddings; (2) *Embedding Richness*, computing mean within-vector standard deviation across dimensions on raw embeddings; and (3) *Semantic Separation*, calculating within-minus-between mean cosine similarity on L2-normalized embeddings using heuristic acoustic classes. Higher values indicate better performance for all metrics.

---

<sup>2</sup>[Link to large glass fishbowl audio sample.](#)

Table 2 presents top-performing configurations from four architecture families: T5 (Raffel et al., 2020), BERT (Devlin et al., 2018), DeBERTa (He et al., 2020), and CLAP (Elizalde et al., 2023). Each architecture is shown with its best pooling strategy from preliminary experiments. Due to space constraints, we report only the highest-performing variant from each model family among 15+ total configurations evaluated.

Error Type	Baseline	XL, Long	XL, Short	L, Long	L, Short	B, Long	B, Short	S, Long	S, Short
Mean Error (%)	-37.0	8.8	4.8	24.6	26.0	30.2	27.7	43.4	21.9
Median Error (%)	-59.6	-33.95	-38.5	-19.0	-23.9	-16.7	-18.6	-10.4	-23.6

**Table 1** RT60 estimation error analysis (n=1957). Negative values indicate underestimation.

Configuration	Batch Div.	Embed. Rich.	Sem. Sep.
T5-Base + First	0.228	0.281	0.079
T5-Large + First	0.163	0.219	0.095
DeBERTa-v3 + Max	0.279	1.682	0.003
BERT-Base + Max	0.235	0.390	0.010
CLAP	0.125	0.290	0.050

**Table 2** Text encoder evaluation for reverb-prompt embeddings across diversity and semantic separation metrics.

**VAE Reconstruction Quality.** Many impulse response generation work operate on spectrogram or mel-spectrogram space, then use Griffin-Lim to recover the phase information (Steinmetz, 2018). As such, we evaluate our VAE against two Griffin-Lim baselines (Griffin and Lim, 1984): reconstruction from mel-spectrograms (GL-Mel) and from STFT magnitudes (GL-STFT). Table 3 presents the evaluation results. Our VAE demonstrates superior time-domain reconstruction fidelity with SNR of  $-0.75$  dB compared to  $-5.26$ – $-5.30$  dB for Griffin-Lim variants, and MSE of  $2.83 \times 10^{-4}$  versus  $7.49$ – $7.62 \times 10^{-4}$ . Additionally, the VAE achieves approximately  $62\times$  faster inference speed, enabling real-time applications. While the VAE exhibits higher RT60 error (mean 6.51%), this represents substantial improvement from initial training (7.26%), indicating learned acoustic modeling capabilities beyond simple magnitude preservation (Le Roux et al., 2019; Schroeder, 1965).

**Comparison with Baseline Methods.** Table 4 analyzes RT60 predictions across the full test set (n=1957). Image2Reverb severely underestimates reverberation, achieving mean RT60 of 1.274 seconds (61.4% deviation from ground truth 3.299 seconds) with constrained maximum of 2.685 seconds and reduced variance (0.535 seconds std). PromptReverb demonstrates superior acoustic modeling with clear scaling effects. The XL model achieves optimal performance: 2.189 seconds for long prompts (29.3% deviation) and 2.044 seconds for short prompts (34.0% deviation). Notably, larger models excel with long prompts while smaller models perform better with short prompts. All PromptReverb variants exhibit realistic dynamic range (maximum values 4.888–5.619 seconds vs. ground truth 5.819 seconds) and variance (1.231–1.427 seconds std vs. ground truth 1.715 seconds), substantially outperforming Image2Reverb’s constrained predictions and indicating faithful representation of diverse acoustic environments.

Following (Singh et al., 2021), we compute RT60 errors as signed percentage deviations from ground truth. Table 1 compares four PromptReverb model scales against Image2Reverb across the full test set, including S: 213M / 0.8GB / 1.9GB (12, 512, 8), B: 329M / 1.3GB / 2.4GB (16, 768, 12), L: 616M / 2.4GB / 3.6GB (24, 1024, 16), XL: 1.5B/ 5.9GB/ 7.7GB (32, 1536, 24), where the format shows params / RAM / model size and the triplet shows (depth, hidden-size, num\_heads). Image2Reverb consistently underestimates RT60 with  $\sim -37\%$  mean error. PromptReverb shows strong scaling effects: S model (43.4% long, 21.9% short), B model (30.2% long, 27.7% short), L model (24.6% long, 26.0% short), and XL model achieving breakthrough performance (8.8% long, 4.8% short). The XL variant’s near ground-truth accuracy across both prompt lengths significantly outperforms Image2Reverb and smaller models.

### 3.3 Subjective Experiments

To complement our quantitative analysis, we conducted a subjective evaluation with human listeners. Nine participants evaluated reverb quality and text-audio matching across three samples: ground truth recordings, Image2Reverb generations, and our PromptReverb method. Each participant rated 24 examples using a 5-point Likert scale, where 1 indicates "Very Poor" and 5 indicates "Excellent" quality or matching. Each trial presented a text description of the

	SNR (dB) $\uparrow$	MSE $\downarrow$	RT60 (%) $\downarrow$	Time (ms) $\downarrow$
VAE (Ours)	-0.75	2.83	6.51	9.8
GL-Mel	-5.26	7.49	58.18	610.7
GL-STFT	-5.30	7.62	0.19	604.9

**Table 3** Comparison of Reconstruction Quality (means over  $n=1957$ ). MSE is reported in units of  $10^{-4}$ .

Method	Mean (s)	Median (s)	Max (s)
Ground-Truth	3.299	3.106	5.819
Image2Reverb (Singh et al., 2021)	1.295	1.211	2.685
<i>PromptReverb</i>			
XL, long	2.189	2.042	5.619
XL, short	2.044	1.793	5.261
L, long	2.470	2.454	5.472
L, short	2.378	2.371	5.526
B, long	2.545	2.431	5.455
B, short	2.472	2.422	5.236
S, long	2.703	2.681	5.516
S, short	2.391	2.323	5.249

**Table 4** RT60 reverberation time vs. model size scaling (n=1957).

acoustic environment, followed by dry audio and three corresponding wet versions (reverberant). Participants rated each sample on two dimensions: overall reverb quality and how well the reverb matched expectations from the text.

Statistical analysis using paired t-tests revealed *PromptReverb*’s advantages. For reverb quality, our method achieved  $3.79 (\pm 0.92)$  versus ground truth  $(3.32 \pm 1.24)$  and Image2Reverb  $(3.51 \pm 1.09)$ . While statistically significant ( $p < 0.05$ ) against both, high standard deviations and small sample size make claimed superiority over real recordings questionable; however, the consistent improvement over Image2Reverb serves as a distant validation of the effectiveness of our approach. For text-audio matching, *PromptReverb* scored  $3.50 (\pm 0.98)$  compared to ground truth  $(2.97 \pm 1.21)$  and Image2Reverb  $(3.26 \pm 1.06)$ . Despite statistical significance against ground truth ( $p < 0.05$ ), large variance warrants cautious interpretation. Figure 2 presents complete evaluation results.

## 4 Conclusion

We introduced *PromptReverb*, a two-stage framework that generates full-band RIRs from natural language descriptions. Our  $\beta$ -VAE achieves superior time-domain reconstruction; the rectified flow DiT generates acoustically accurate RIRs with 8.8% mean RT60 error, outperforming Image2Reverb’s  $-37\%$  underestimation. Human evaluation confirms improved perceptual quality (3.79 vs. 3.51) while maintaining text-audio semantic alignment. *PromptReverb* represents the first system capable of synthesizing perceptually convincing 48 kHz RIRs from free-form text, eliminating requirements for panoramic imagery or technical acoustic expertise. This enables practical applications in VR/AR, game audio, and architectural acoustics where intuitive RIR generation is essential.

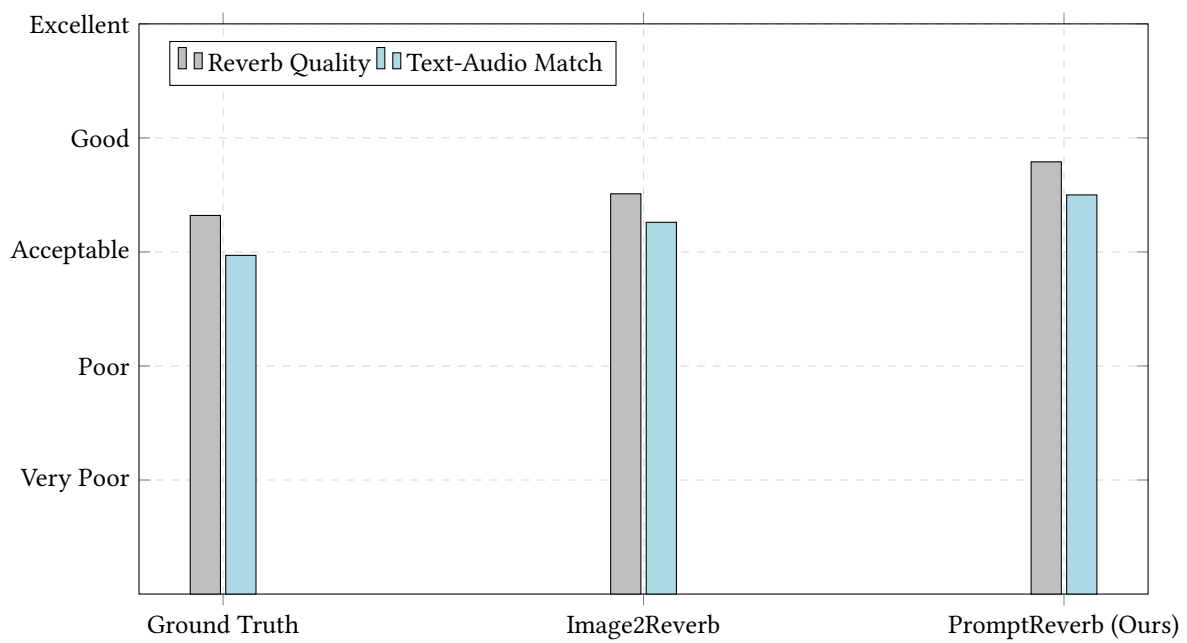


**Figure 2** Subjective evaluation results showing mean ratings for reverb quality and text-audio matching. PromptReverb outperforms ground truth on both measures and Image2Reverb on quality.

## References

Jont B Allen and David A Berkley. Image method for efficiently simulating small-room acoustics. *J. Acoust. Soc. Am.*, 65(4):943–950, 1979.

Anthropic. Claude opus 4.1: Enhanced reasoning and multimodal capabilities, 2024.

Silvia Arellano, Chunghsin Yeh, Gautam Bhattacharya, et al. Room impulse response generation conditioned on acoustic parameters. *arXiv preprint arXiv:2507.12136*, 2025.

Changan Chen, Carl Schissler, Sanchit Garg, et al. Soundspaces 2.0: A simulation platform for visual-acoustic learning. *NeurIPS*, 2022.

Gheorghe Comanici, Eric Bieber, Mike Schaekermann, et al. Gemini 2.5: Advanced reasoning, multimodality, and long context capabilities. *arXiv preprint arXiv:2507.06261*, 2025.

Miguel de la Torre, Marco Comunità, Alexander Rixen, et al. Diffusionrir: Room impulse response interpolation using diffusion models. *arXiv preprint arXiv:2504.20625*, 2024.

Jacob Devlin, Ming-Wei Chang, Kenton Lee, and Kristina Toutanova. Bert: Pre-training of deep bidirectional transformers for language understanding. *arXiv preprint arXiv:1810.04805*, 2018.

Benjamin Elizalde, Soham Deshmukh, Mahmoud Al Ismail, et al. Clap: Learning audio concepts from natural language supervision. *arXiv preprint arXiv:2206.04769*, 2023.

Daniel Griffin and Jae Lim. Signal estimation from modified short-time fourier transform. *IEEE Trans. Acoust. Speech Signal Process.*, 32(2):236–243, 1984.

Kaiming He, Xiangyu Zhang, Shaoqing Ren, et al. Deep residual learning for image recognition. In *Proc. CVPR*, pages 770–778, 2016.

Pengcheng He, Xiaodong Liu, Jianfeng Gao, et al. Deberta: Decoding-enhanced bert with disentangled attention. *arXiv preprint arXiv:2006.03654*, 2020.

Irina Higgins, Loic Matthey, Arka Pal, et al. Beta-vae: Learning basic visual concepts with a constrained variational framework. In *Proc. ICLR*, 2017.

Shengpeng Ji, Ziyue Jiang, Xize Wang, et al. Wavtokenizer: An efficient acoustic discrete codec tokenizer for audio language modeling. *arXiv preprint arXiv:2408.16532*, 2024.

Tom Ko, Vijayaditya Peddinti, Daniel Povey, et al. A study on data augmentation of reverberant speech for robust speech recognition. In *Proc. ICASSP*, 2017.

Jungil Kong, Jaehyeon Kim, and Jaekyoung Bae. Hifi-gan: Generative adversarial networks for efficient and high fidelity speech synthesis. *Advances in Neural Information Processing Systems*, 33:17022–17033, 2020.

Asbjørn Krokstad, Svein Strøm, and Sigurd Sørdsdal. Calculating the acoustical room response by the use of a ray tracing technique. *J. Sound Vib.*, 8(1):118–125, 1968.

Jonathan Le Roux, Scott Wisdom, Hakan Erdogan, et al. A blueprint for a real-time speech codec with neural vocoders. In *Proc. IEEE WASPAA*, pages 8–12, 2019.

Susan Liang, Chao Huang, Yapeng Tian, et al. Language-guided joint audio-visual editing via one-shot adaptation. In *Proc. Asian Conf. Computer Vision*, pages 1011–1027, 2024.

Marco Lin, Vesa Välimäki, and Sebastian J. Schlecht. Deep room impulse response completion. *EURASIP J. Audio Speech Music Process.*, 2024:1–15, 2024.

Xingchao Liu, Chengyue Gong, and Qiang Liu. Rectified flow: A marginal preserving approach to optimal transport. *arXiv preprint arXiv:2209.14577*, 2022a.

Xiulong Liu, Anurag Kumar, Paul Calamia, et al. Hearing anywhere in any environment. In *Proc. CVPR*, pages 5732–5741, 2025.

Zhuang Liu, Hanzi Mao, Chao-Yuan Wu, et al. A convnet for the 2020s. In *Proc. CVPR*, pages 11976–11986, 2022b.

Sheng Lyu, Yuemin Yu, and Chenshu Wu. Temporal modeling of room impulse response generation via multi-scale autoregressive learning. In *Proc. Interspeech*, pages 923–927, 2025.

Mistral AI. Mistral medium 3.1: Efficient large language models, 2024.

Damian T Murphy. Openair: The open acoustic impulse response library. University of York, 2010.

OpenAI. Gpt-4o: Improved multimodal capabilities, 2024a.

OpenAI. Gpt-5: Advanced language understanding and generation, 2024b.

William Peebles and Saining Xie. Scalable diffusion models with transformers. In *Proc. ICCV*, pages 4195–4205, 2023.

Colin Raffel, Noam Shazeer, Adam Roberts, Katherine Lee, Sharan Narang, Michael Matena, Yanqi Zhou, Wei Li, and Peter J Liu. Exploring the limits of transfer learning with a unified text-to-text transformer. *Journal of Machine Learning Research*, 21(140):1–67, 2020.

Anton Ratnarajah, Shi-Xiong Tang, and Dinesh Manocha. Mesh2ir: Neural acoustic impulse response generator for complex 3d scenes. In *Proc. ACM Multimedia*, pages 6010–6018, 2022a.

Anton Ratnarajah, Shi-Xiong Tang, and Dinesh Manocha. Fast-rir: Fast neural diffuse room impulse response generator. In *Proc. ICASSP*, pages 571–575, 2022b.

Anton Ratnarajah, Shi-Xiong Tang, Sreyan Athar, et al. Av-rir: Audio-visual room impulse response estimation. In *Proc. CVPR*, pages 9544–9554, 2024.

Microsoft Research. Phi-4 technical report. <https://huggingface.co/microsoft/phi-4>, 2024.

Jessie Richter-Powell, Antonio Torralba, and Jonathan Lorraine. Score distillation sampling for audio: Source separation, synthesis, and beyond. *arXiv preprint arXiv:2505.04621*, 2025.

Robin Scheibler, Eric Bezzam, and Ivan Dokmanić. Pyroomacoustics: A python package for audio room simulations and array processing algorithms. In *Proc. ICASSP*, 2018.

Manfred R. Schroeder. New method of measuring reverberation time. *J. Acoust. Soc. Am.*, 37(3):409–412, 1965.

Nikhil Singh, Jeff Menth, Jerry Ng, et al. Image2reverb: Cross-modal reverb impulse response synthesis. In *Proc. ICCV*, pages 286–295, 2021.

Christian Steinmetz. Neuralreverberator. 2018.

Rebecca Stewart and Mark Sandler. Database of omnidirectional and b-format impulse responses. In *Proc. ICASSP*, 2010.

Ashish Vaswani, Noam Shazeer, Niki Parmar, et al. Attention is all you need. *NeurIPS*, 2017.

Vikram Voleti, Chris Scarvelis, Lyndon Duong, et al. Moondream: A vision language model for general purpose visual instruction following. *arXiv preprint arXiv:2311.06607*, 2023.

Vikram Voleti et al. Moondream: A vision language model for real-world understanding. <https://huggingface.co/vikhyatk/moondream2>, 2024.

Peng Wang, Shuai Bai, Sinan Tan, et al. Qwen2-vl: Enhancing vision-language model’s perception of the world at any resolution. *arXiv preprint arXiv:2409.12191*, 2024.

Yiming Zhang, Xiangdong Chen, Hong-Yu Zhou, et al. Mean-rir: Multi-modal environment-aware network for robust room impulse response estimation. *arXiv preprint arXiv:2509.05205*, 2025.

Junhui Zhao, Hang Chen, Qing Wang, et al. Ta-rir: Topology-aware neural modeling of acoustic propagation for room impulse response synthesis. In *Proc. Interspeech*, pages 2485–2489, 2025.